JACS
JOURNAL OF THE AMERICAN CHEMICAL SOCIETY
pubs.acs.org/JACS
Article

Can the Hock Process Be Used to Produce Phenol from Polystyrene?

Doohyun Baek, Abdullah J. Al Abdulghani, Dylan J. Walsh, Dillon T. Hofsommer, James B. Gerken, Changxia Shi, Eugene Y.-X. Chen, Ive Hermans,* and Shannon S. Stahl*

Cite This: J. Am. Chem. Soc. 2025, 147, 8687−8694
Read Online

ABSTRACT: Polystyrene (PS) is a widely used thermoplastic polymer, but its very low recycling rate has motivated consideration of chemical conversion strategies to convert waste PS into value-added products. Oxidation methods have been widely studied, but they typically generate benzoic acid, a product with a relatively low market demand. Phenol is a higher volume chemical that would be an appealing target, but no methods currently exist for the conversion of PS into phenol. The repeat unit in PS closely resembles cumene, the primary feedstock used to produce phenol through the Hock process. Here, we investigate prospects for adapting the Hock process to PS, generating hydroperoxides through the autoxidation of benzylic C−H bonds followed by the acid-promoted rearrangement of the hydroperoxides to afford phenol and a partially oxygenated polymer. Experimental and computational studies of dimeric and trimeric PS model compounds show that neighboring phenyl rings impose conformational constraints that raise the barrier to hydrogen-atom transfer from the tertiary benzylic C−H bond. These effects are also evident with PS and contribute to lower yields of phenol when PS is subjected to Hock process conditions. These results provide valuable insights that have important implications for other efforts that seek to adapt small-molecule reactivity to polymeric feedstocks.

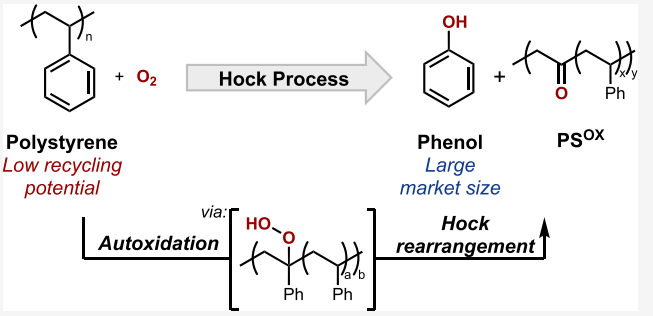

INTRODUCTION

Polystyrene (PS) is an inexpensive, large-volume commodity polymer used in applications ranging from packaging to insulation and consumer goods.[1] Most postconsumer PS, however, ends up in landfills and has a recycling rate of less than 1%.[2−4] Various chemical recycling strategies are being considered for the conversion of waste PS into valuable products.[5−7] Much of this effort has focused on thermochemical approaches, such as gasification[8] and pyrolysis,[9] or reduction methods, such as hydrogenolysis[10] and hydrocracking.[11] Oxidation methods, particularly those using O_2 as the oxidant, represent an alternative strategy. These thermodynamically favorable reactions require little energy input and can directly access valuable products that can reenter the chemical value chain.[12]

Industrial methods for hydrocarbon oxidation offer a valuable starting point for consideration of conditions for waste plastics valorization. For example, the mid-century (MC) process,[13] an industrial Co/Mn/Br-catalyzed autoxidation method for the conversion of *p*-xylene into terephthalic acid (Figure 1a), has been applied to individual and mixed polymer feedstocks.[14−17] These and other thermal[18−21] and photochemical[22−31] oxidation conditions typically convert PS into benzoic acid. While these reactions often proceed with high selectivity, the market demand for benzoic acid[31] is relatively small (Figure 1b). Biological conversion offers a potential strategy to use benzoic acid as a feedstock for the production of value-added products,[15,16] but chemical methods to convert PS into products other than benzoic acid merit attention.[32] Phenol has a much larger market volume than benzoic acid, but methods for the conversion of PS to phenol have not yet been reported. Phenol is currently produced in the multistep Hock process, which involves autoxidation of cumene and subsequent acid-promoted rearrangement of cumene hydroperoxide to yield phenol and acetone (Figure 1c).[33] The structural similarity between the repeat unit in PS and cumene raises the prospect that the Hock process could be adapted to produce phenol from PS. Here, we explore this possibility. The data show that the autoxidation and acid-promoted rearrangement reactivity change significantly when dimeric and trimeric PS subunits are used instead of cumene. Experimental and computational studies reveal that proximal phenyl groups along the backbone hinder both steps and limit the hydroperoxide and phenol yields. Higher molecular weight derivatives, including pentamers and PS itself, closely resemble the behavior of the trimeric compound. Treatment of PS under Hock process conditions affords phenol and a partially

Received: December 18, 2024
Revised: February 5, 2025
Accepted: February 6, 2025
Published: February 26, 2025

https://doi.org/10.1021/jacs.4c18143
J. Am. Chem. Soc. 2025, 147, 8687−8694

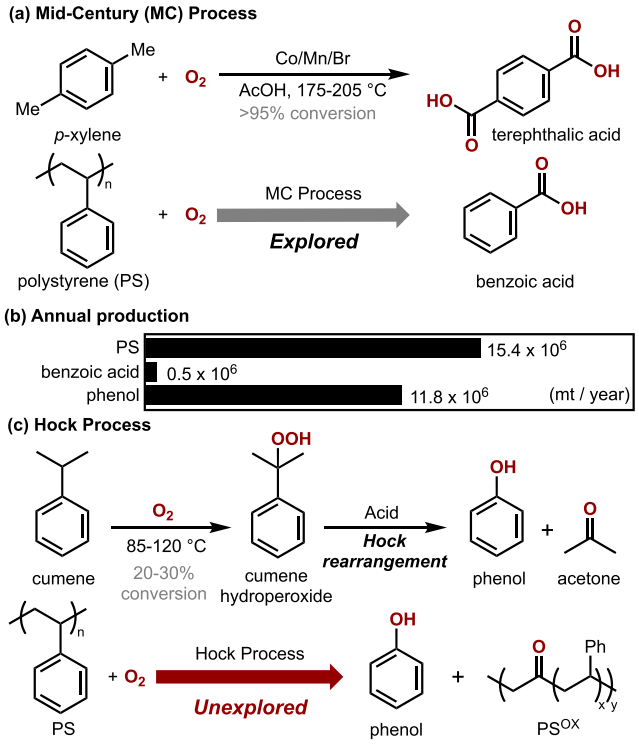

Figure 1. (a) Mid-century process for production of terephthalic acid from *p*-xylene and its extension to polystyrene conversion to benzoic acid. (b) Market size of relevant chemicals. (c) Cumene oxidation/rearrangement in the Hock process, with targeted adaptation to polystyrene as a feedstock for phenol production.

oxidized polymeric byproduct (PS^{OX}, see Figure 1c) that retains phenyl groups. The latter material can be used to produce benzoic acid under MC conditions, and the tandem Hock/MC oxidation sequence provides a means to access both phenol and benzoic acid from waste PS. More broadly, this work provides important fundamental insights relevant to the adaptation of commodity-scale oxidation conditions to waste-plastic feedstocks.

RESULTS AND DISCUSSION

Autoxidation of Dimeric and Trimeric PS Model Compounds. The industrial autoxidation of cumene (**1**) to cumene hydroperoxide (**1a**) is typically carried out in neat cumene around 135 °C, achieving a single-pass conversion of approximately 20−30%.[33−35] These conditions are unsuitable for reactions with PS, as both hydroperoxides and unreacted C−H sites remain on the same polymer chain, complicating the recovery and recycling of the unreacted material. Consequently, we considered alternative conditions for cumene autoxidation that use organic solvents and radical initiators, which enable higher conversion to cumene hydroperoxide.[36−40] Ishii and coworkers used acetonitrile as the solvent, with NHPI (*N*-hydroxyphthalimide) and AIBN (azobis(isobutyronitrile)) as radical initiators, to convert cumene to cumene hydroperoxide with 76% conversion and 75% yield.[36] This method has been the focus of industrial interest and further development.[38−40] Validation of these results in our own laboratory (see Figure S5) motivated us to explore conditions of this type for reactions with PS.

We elected to initiate our study by investigating the dimeric and trimeric PS model compounds *trans*-**2** and **3** (the latter as a mixture of diastereomers) (Figure 2). These compounds provide a structural bridge between cumene and PS and enable more straightforward analysis of autoxidation products relative to reactions with PS. Reactivity studies began by evaluating the autoxidation of **2** and **3** in acetonitrile in the presence and absence of various hydrogen-atom transfer reagents (e.g., NHPI, *t*BuOOH, and *t*BuOO*t*Bu) and radical initiators (e.g., AIBN and $Co(OAc)_2$). These screening studies showed that conditions similar to those reported by Ishii afforded the highest yields of hydroperoxides derived from **2** and **3** (see Section 4a in Supporting Information for details). The dimeric compound **2** undergoes selective conversion to the bis-hydroperoxide **2a** (as a mixture of diastereomers), with the monohydroperoxide forming in only trace amounts (<1%). Most of the remaining mass balance is present as unreacted dimer **2** (see Supporting Information for analytical details). TPNHPI (tetraphenyl-*N*-hydroxyphthalimide) gives better yields of **2a** than NHPI, while both reactions benefit from the presence of AIBN (31% vs 20% yield, respectively; see Figure 2a, entry 1 and Figure S12 in Supporting Information). PS is not soluble in acetonitrile, while NHPI has poor solubility in nonpolar solvents. Valeronitrile (^{n}BuCN) offers a suitable compromise and led to an improved yield of *bis*-hydroperoxide **2a** (40%, Figure 2a, entry 2).

Small amounts of acetophenone (**4**, 2.0 mol %) and α-methylstyrene (**5**, 0.5 mol %) are observed as side products in these reactions (Figure 2a). Control experiments show that α-methylstyrene inhibits autoxidation of the dimeric substrate *trans*-**2** (Figure 2b), likely by trapping reactive radical intermediates (see Section 3e in Supporting Information for additional details). This observation prompted us to consider the mechanistic origin of α-methylstyrene (and acetophenone) formation during the reaction of **2** (Figure 2c). The bis-hydroperoxide is proposed to arise from rapid intramolecular 1,5-hydrogen-atom transfer (HAT) from the initial peroxyl radical intermediate **Int-B**. The resulting tertiary radical intermediate can then react with O_2 (path I, Figure 2c) or undergo the O_2-independent O−O/C−C cleavage step to afford α-methylstyrene and acetophenone (path II, Figure 2c). This hypothesis suggested that improved conversion to the bis-hydroperoxide should be accessible at higher O_2 pressure. With 10 atm O_2,[41] a 56% yield of bis-hydroperoxide **2a** was obtained without α-methylstyrene generation (entry 3). The acetophenone formed under these conditions can arise from the decomposition of **2a** (i.e., different from path II). When the reaction temperature is increased from 70 to 100 °C, the conversion of **2** increased, but the yield of **2a** decreased and the yield of acetophenone increased (Figure 2a, entry 4).

The reactivity of trimeric model compound **3** shows the influence of an additional monomer unit. Under conditions optimized with **2**, the reaction of **3** generates hydroperoxides exclusively at the terminal tertiary benzylic positions, yielding monohydroperoxide **3a** in 23% yield and bis-hydroperoxide **3b** in 24% yield (Figure 2a, entry 5). A small amount of ketone **6** and acetophenone was observed as side products. Overall, these observations indicate that the trimer has a lower reactivity than the dimer.

Computational Studies. Density functional theory (DFT) calculations were performed to assess the energetics of the oxidation pathways of dimer and trimer model compounds **2** and **3** in order to gain insight into their different reactivity. Figure 3 highlights the steps that show significant differences between the two compounds, including (a) PINO-

https://doi.org/10.1021/jacs.4c18143
J. Am. Chem. Soc. 2025, 147, 8687−8694

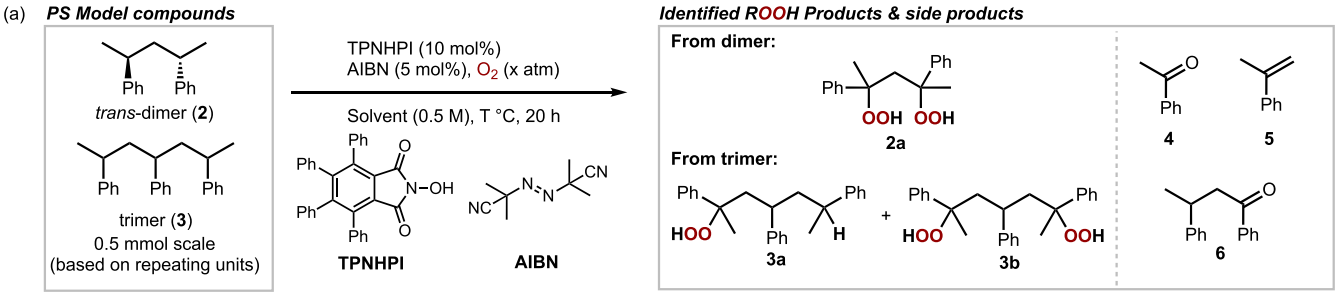

Entry	Substrates	O_2 condition	T [°C]	Conv. [%][a]	Solvent	ROOH [%][b] 2a	3a	3b	ROOH [%][c] per # of Ph	side products [%] 4	5	6
1	Dimer (**2**)	O_2, 1 atm	70	39	MeCN	31	-	-	31	1.6	0.3	-
2	Dimer (**2**)	O_2, 1 atm	70	45	^{n}BuCN	40	-	-	40	2.0	0.5	-
3	Dimer (**2**)	O_2, 10 atm	70	74	^{n}BuCN	56	-	-	56	3.7	-	-
4	Dimer (**2**)	O_2, 10 atm	100	82	^{n}BuCN	50	-	-	50	8.6	-	-
5	Trimer (**3**)	O_2, 10 atm	70	56	^{n}BuCN	-	23	24	24	1.3	-	2.7

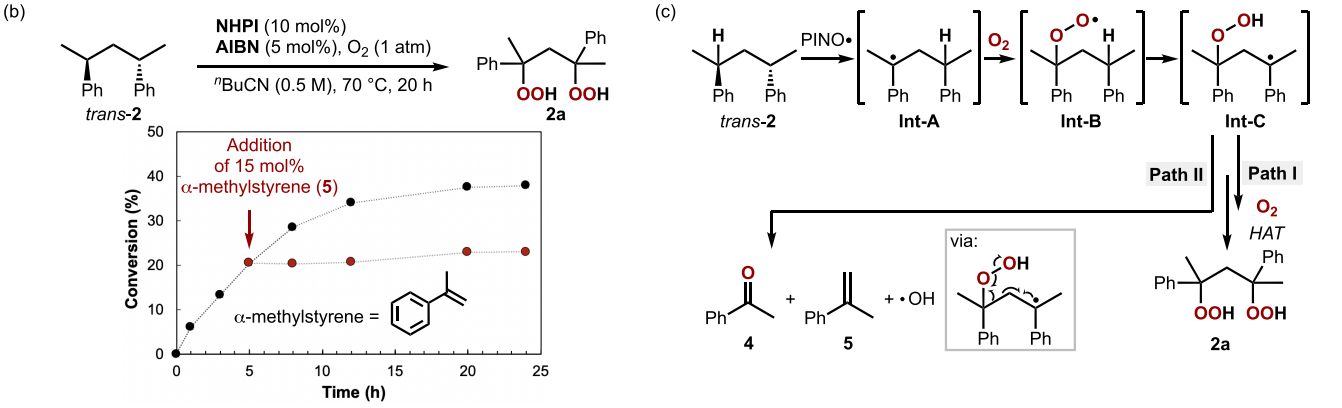

Figure 2. (a) Autoxidation optimization with polystyrene model compounds **2** and **3**. Reaction conditions: 0.5 mmol of Ph-containing subunits (0.25 mmol **2** and 0.167 mmol **3**), 10 mol % TPNHPI (tetraphenyl-*N*-hydroxyphthalimide), 5 mol % AIBN (azobis(isobutyronitrile)), O_2 (1 or 10 atm), and 1 mL valeronitrile (^{n}BuCN) at 70 or 100 °C. [a]Conversion of **2** or **3**. [b]Yield of ROOH products **2a**, **3a**, or **3b** was analyzed by UPLC as alcohols obtained by reduction with PMe_3. [c]Yield of ROOH products recalculated based on peroxides per the number of phenyl rings. (b) Inhibitory effect of α-methylstyrene in the autoxidation reaction of **2**. (c) Proposed mechanisms for the O_2-dependent formation of **2** (path I) and formation of acetophenone **4** and α-methylstyrene **5** (path II).

mediated HAT to form the tertiary benzylic radical and (b) intramolecular HAT from the intermediate peroxyl radical (see Section 5 of Supporting Information for the full reaction pathway). Hydrogen-atom transfer (HAT) from a benzylic C−H bond in **2** exhibits an energy barrier of 24.9 kcal/mol (**TS-A**, Figure 3a) in the formation of benzylic radical intermediate **Int-A**. In the reaction of **3**, two potential PINO-mediated HAT pathways were considered: one from a terminal benzylic C−H bond and the other from an internal benzylic C−H bond. Reaction of PINO with the terminal C−H bond forms the benzylic radical intermediate **Int-1** with an energy barrier of 26.4 kcal/mol (**TS-1**), while reaction with the internal C−H bond to form **Int-1'** has a higher energy barrier of 33.3 kcal/mol (**TS-1'**). Each of these radicals undergoes a barrierless reaction with O_2 to afford peroxyl radical species (Figure S16 in Supporting Information).

Intramolecular HAT by the dimeric and trimeric peroxyl radical intermediates **Int-B** and **Int-2** (Figure 3b) initiates stepwise formation of the bis-hydroperoxide products **2a** and **3b** (cf. Figure 2). Comparison of the 1,5-HAT energy barriers for these intermediates shows that the reaction of the trimer has a 2.2 kcal/mol higher energy barrier than the reaction of the dimer (**TS-2'** versus **TS-B**). The trimer, however, can also undergo 1,7-HAT through the transition state **TS-2**. The results show that 1,7-HAT is favored by 2.3 kcal/mol over the 1,5-HAT step. Together, this analysis of inter- and intramolecular HAT energetics rationalizes the lack of C−H oxidation products arising from HAT at the central benzylic C−H bond of the trimer (cf. Figure 2).

Optimization of the Acid-Promoted Hock Rearrangement. Subsequent efforts focused on the acid-promoted reaction of hydroperoxides **2a**, **3a**, and **3b** obtained from the autoxidation reaction, without purification (the hydroperoxides present safety hazards and are insufficiently stable to isolate in pure form). Each reaction was conducted with 0.2 mmol of total hydroperoxide, and the yields were recorded with respect to the hydroperoxide content. Initial tests probed the reaction of **2a** with various Brønsted and Lewis acids (Figures 4 and S15). Lewis acids generally led to lower phenol yields compared to reactions with Brønsted acids, and the highest phenol yields were obtained with the strong acids, sulfuric acid (H_2SO_4, 53% yield) and perchloric acid ($HClO_4$, 58% yield) (Figure 4, entries 1 and 2). Increased acid concentration enhanced the yield (entries 3 and 4), and the best outcome was observed with 3.6 M perchloric acid ($HClO_4$) in MeCN, affording phenol in 72% yield with respect to the hydro-

https://doi.org/10.1021/jacs.4c18143
J. Am. Chem. Soc. 2025, 147, 8687−8694

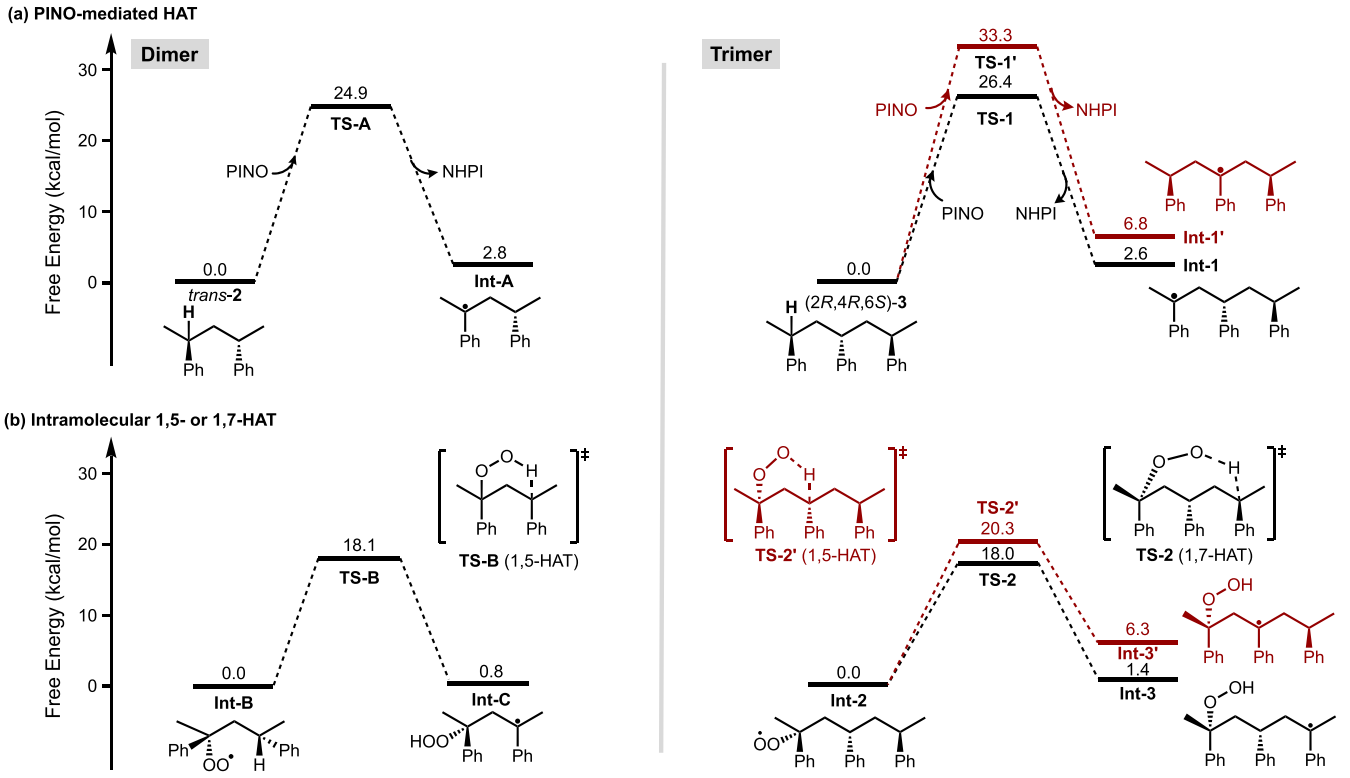

Figure 3. Computational data for the oxidation pathways of the dimer and trimer. Density functional theory (DFT) calculations were performed using the B3LYP exchange-correlation functional as implemented in Gaussian 16 using the 6-311++G(df,pd) basis set. The *trans*-dimer **2** and (2*R*,4*R*,6*S*)-trimer **3** were selected for calculation among the diastereomers.

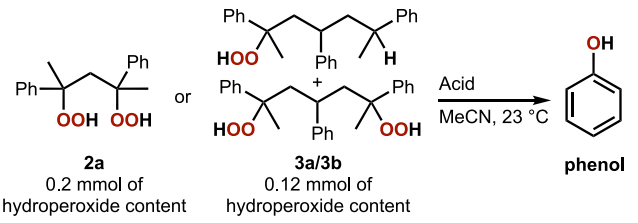

Entry	Substrates	Acid treatment (in 1 mL of MeCN)	Phenol Yield [%] (two-step yield)
1	**2a**	H_2SO_4 0.30 M	53 (21)
2	**2a**	$HClO_4$ 0.30 M	58 (24)
3	**2a**	H_2SO_4 3.6 M	62 (25)
4	**2a**	$HClO_4$ 3.6 M	72 (30)
5	**3a/3b**	$HClO_4$ 3.6 M	71 (17)

Figure 4. Acid-promoted Hock rearrangement conditions with crude **2a** and **3a**/**3b** obtained from autoxidation of **2** and **3** (cf. Figure 2a). The yield of phenol was analyzed by UPLC. The yield in parentheses is the two-step yield from **2** or **3**.

peroxide content (Figure 4, entry 4). Similar performance was observed with the mixture of mono- and bis-hydroperoxide species, which afforded a 71% yield of phenol (Figure 4, entry 5).

Hock Process Applied to PS. The above studies of model compounds provided the basis for the analysis of PS under the same sequential oxidation/acid-promoted rearrangement conditions. Subjecting PS (M_n ~ 73 kDa) to the optimized autoxidation conditions led to the incorporation of hydroperoxides at approximately 25 mol % of the benzylic positions in the PS backbone (**PS**^{OOH}, Figure 5a). The hydroperoxide content was estimated by reducing the hydroperoxides with triphenylphosphine (PPh_3) and quantifying the resulting triphenylphosphine oxide ($Ph_3P{=}O$) by UPLC. This titration method was validated by performing the same assay with bis-hydroperoxide **2a**, which can be independently quantified by other methods (see Section 6b of Supporting Information for details). ^{1}H NMR spectroscopic analysis of **PS**^{OOH} does not reveal the presence of alkene or carbonyl groups, similar to the formation of α-methylstyrene and acetophenone with the dimeric model compound (cf. Figures 2a and S18); however, a small C=O stretching peak at 1716 cm^{-1} is evident in an IR spectrum, suggesting that small quantities of terminal benzoyl groups may be present (Figure 5c).

Subjecting the PS-hydroperoxide material to the optimized acid treatment conditions led to a 52% yield of phenol with respect to the hydroperoxide content (Figure 5a), corresponding to a 12.7% yield with respect to phenyl rings in the original PS sample. Other products, including benzoic acid (1.6% yield) and acetophenone (1.3% yield), were formed in only small quantities, showing that phenol is the major product formed upon treatment of PS under Hock process conditions. The same reaction sequence performed with various sources of postconsumer PS afforded similar yields of phenol (10−12%, Figure S24), indicating that this approach could be extended to waste plastic materials.

Gel permeation chromatographic analysis of the polymer during the autoxidation step revealed that the molecular weight of PS progressively decreased from 73 to 2 kDa during the reaction (Figure 5b). These observations are consistent with chain scission occurring during the reaction, likely resembling observations made with the well-defined model compounds (cf. compounds **4**−**6** in Figure 2). A further decrease in

https://doi.org/10.1021/jacs.4c18143
J. Am. Chem. Soc. 2025, 147, 8687−8694

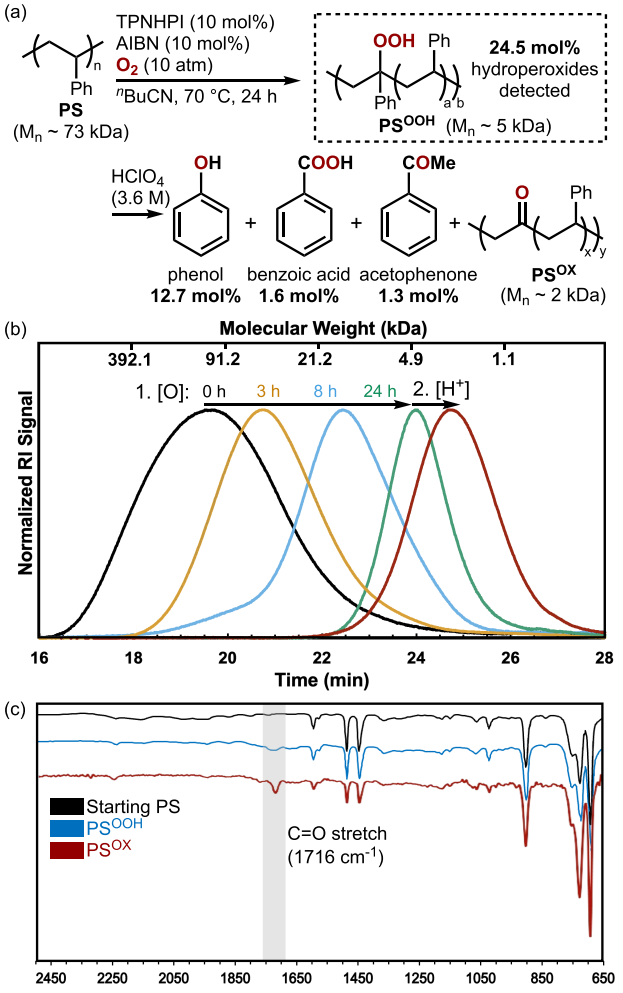

Figure 5. (a) Application of the optimized Hock process conditions to polystyrene. Reaction conditions: 1.0 mmol of Ph-containing monomer units in polystyrene, 10 mol % TPNHPI (tetraphenyl-*N*-hydroxyphthalimide), 10 mol % AIBN (azobis(isobutyronitrile)), O_2 (10 atm), and 2 mL valeronitrile (^{n}BuCN) at 70 °C. (b) Gel permeation chromatographic time-course analysis of polystyrene during the oxidation [O] and acid-promoted Hock rearrangement, [H^+]. (c) IR spectra of starting polystyrene and oxidized polystyrene before/after acid treatment.

molecular weight is observed upon treating the oxidized polymer with acid, as would be expected from the release of phenol from the polymer backbone. IR spectroscopic analysis of the starting PS and solids recovered after acid treatment of the oxidized PS showed the appearance of a new peak at 1716 cm^{-1}, consistent with the introduction of carbonyl groups into the polymer backbone (Figure 5c).

Further Conversion of Oxidized PS to Oxygenated Aromatic Monomers. The above data indicate that treatment of PS under Hock process conditions leads to partial conversion to phenol, together with a partially oxidized, low-molecular-weight polymeric byproduct (PS^{OX}). We postulated that the latter material could be subjected to MC oxidation conditions (cf. Figure 1a), similar to those used previously to convert PS to benzoic acid (Figure 6).[15] To test this hypothesis, the PS^{OX} material obtained from the sequential Hock process conditions described above was separated from phenol by precipitation in pentane and washed with methanol. It was then subjected to Co/Mn/NHPI-catalyzed oxidation in

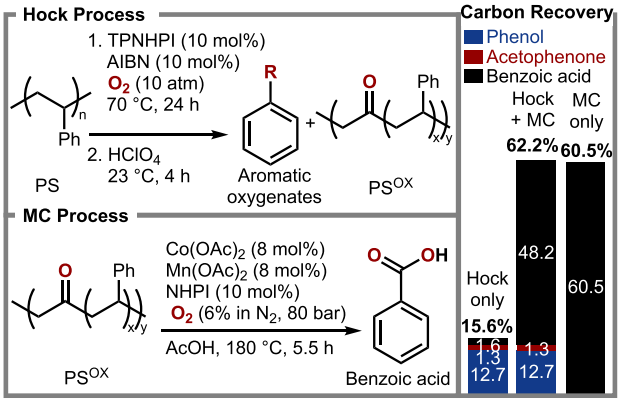

Figure 6. Sequential Hock and MC process. Hock process conditions: 1.0 mmol of PS, 10 mol % TPNHPI (tetraphenyl-*N*-hydroxyphthalimide), 10 mol % AIBN (azobis(isobutyronitrile)), O_2 (10 atm), and 2 mL valeronitrile (^{n}BuCN) at 70 °C. MC process conditions: 1.0 mmol of virgin PS or PS^{OX} after Hock process, 8 mol % of $Co(OAc)_2$, 8 mol % of $Mn(OAc)_2$, 10 mol % of NHPI (*N*-hydroxyphthalimide), 80 bar of 6% O_2 in N_2, and 5 mL of AcOH at 180 °C.

acetic acid, according to the previously reported conditions. This reaction led to a 48% yield of benzoic acid with respect to the phenyl ring present in the original PS (i.e., before the Hock process treatment). This tandem Hock/MC-process sequence afforded 62% total yield of oxygenated aromatic monomers from PS, which may be compared to the 61% yield of benzoic acid obtained when PS is treated directly under the MC conditions (Figure 6).[42] These results show that the PS^{OX} byproduct retains aromatic subunits that may be converted to benzoic acid and further show how the Hock process conditions may be used to divert a significant fraction of the phenyl rings in PS into phenol.

Implications for Adaptation of Small-Molecule Transformations to Polymers. The significance of this work goes beyond the possible practical application noted in Figure 6, as fundamental insights into the relative reactivity of small molecule and polymeric feedstocks have important implications for waste plastics remediation. To bridge the gap between the dimeric/trimeric PS model compounds and PS, we prepared two PS-like oligomers with an average molecular weight corresponding to pentamers and decamers. Both materials have narrow dispersities ($Đ$ = 1.05 and 1.02, respectively), and they were used as substrates under the Hock process conditions to produce phenol (Figure 7). Cumene was also included to establish a benchmark for the reactivity of PS and the PS analogues. The results show that the yield of phenol drops significantly for the dimer, relative to cumene (36% and 70% yield), and another significant decrease is observed between the trimer and dimer (17% and 36%). Further increases in the molecular weight, progressing from trimer to pentamer, decamer, and PS, show relatively modest changes in phenol yield (17%−13%).

The yield of phenol appears to be influenced most strongly by the yield of hydroperoxide in the initial autoxidation step. Although both autoxidation and acid-promoted rearrangement are influenced by the substrate identity, the major role of the autoxidation step is supported by the significant drop in hydroperoxide yield with cumene (77%), dimer (56%), and trimer (24%) (see above). To probe these differences further, we performed competition experiments in which cumene and the dimer or trimer were combined and subjected to

https://doi.org/10.1021/jacs.4c18143
J. Am. Chem. Soc. 2025, 147, 8687−8694

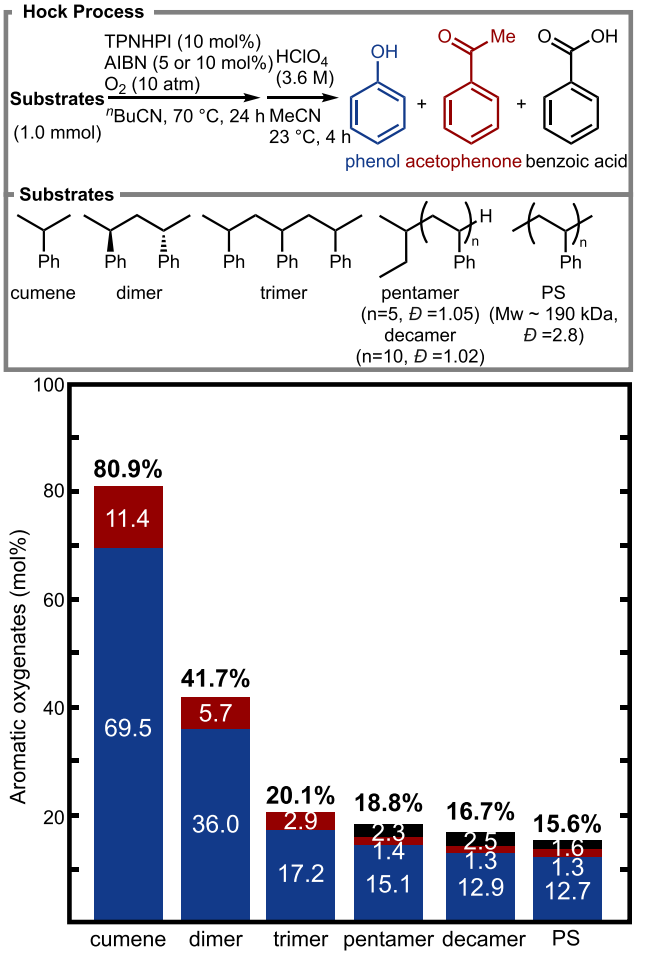

Figure 7. Effectiveness of the Hock process on PS-like compounds ranging from cumene to PS. Hock process conditions: for cumene, dimer, and trimer: 1.0 mmol of substrate, 10 mol % TPNHPI (tetraphenyl-*N*-hydroxyphthalimide), 5 mol % AIBN (azobis(isobutyronitrile)), O_2 (10 atm), and 2 mL valeronitrile (^{n}BuCN) at 70 °C. For pentamer, decamer, and PS: 1.0 mmol of substrates, 10 mol % TPNHPI, 10 mol % AIBN, O_2 (10 atm), and 2 mL valeronitrile (^{n}BuCN) at 70 °C.

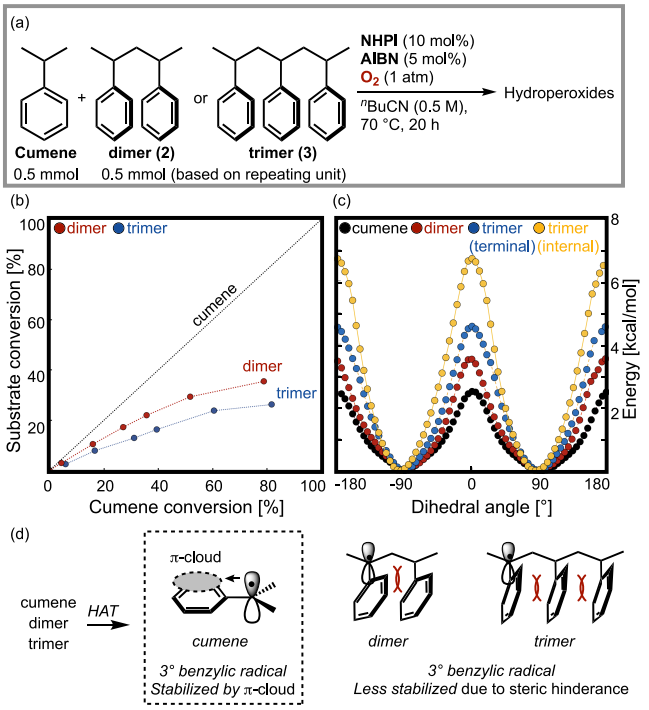

Figure 8. (a) Substrate conversion experiments under the reaction conditions: 0.5 mmol of substrates based on repeating units, 0.5 mmol of cumene, 10 mol % NHPI (*N*-hydroxyphthalimide), 5 mol % AIBN (azobis(isobutyronitrile)), O_2 (1 atm), and 1 mL ^{n}BuCN at 70 °C. (b) The resulting substrate conversion graph under the reaction. (c) Rotational energy barriers for cumene, dimer, and trimer during dihedral angle scans. (d) Benzylic radical stabilization by the phenyl group.

autoxidation conditions (Figure 8a). The conversion of each substrate was monitored, and a plot of the dimer/trimer conversion with respect to cumene conversion is shown in Figure 8b. The data confirm that the relative reactivity of the substrate decreases with increasing chain length, consistent with the computational data in Figure 3a, which reveal a higher activation barrier for PINO-mediated HAT from the trimer relative to the dimer. To explore the origin of these trends, dihedral scans of the phenyl ring were performed with cumene and the dimer and trimer model compounds, and both terminal and internal phenyl rings were evaluated for the trimer (Figure 8c). The lowest energy conformer for each of the structures features a 90° (or 270°) dihedral angle between the plane of the phenyl ring and the plane of the aliphatic backbone, and the highest energy arises when the phenyl ring and backbone are coplanar (0° and 180°). The data in Figure 8c reveal that increasing the number of PS subunits restricts the phenyl ring rotation. The energy of the coplanar conformation increases progressively in the sequence of cumene (2.5 kcal/mol), dimer (3.5 kcal/mol), terminal phenyl rings of the trimer (4.6 kcal/mol), and the internal phenyl ring of the trimer (6.7 kcal/mol). The coplanar conformation stabilizes the benzylic radical generated by HAT, and rotational restrictions contribute to higher HAT barriers (Figure 8d). These insights show that, in spite of the structural similarity between cumene and PS subunits, the presence of adjacent groups in PS has energetic consequences for autoxidation that are not present in cumene. It is reasonable to expect that related considerations could impact other efforts to extend autoxidation reactivity from small molecules to polymers.

■ CONCLUSION

Phenol represents an ideal chemical target for valorization of waste PS. This study introduces a strategy to achieve this goal by subjecting PS to Hock process conditions. The use of well-defined dimeric and trimeric model compounds provides valuable insights into the relationship between cumene, the conventional Hock process substrate, and PS. These compounds permit direct characterization of reaction intermediates and comparison of reaction performance between cumene and PS-like structures. The inclusion of pentameric and decameric PS structures shows progressive reactivity that links the well-defined model compounds to PS. Experimental and computational studies reveal that the phenol yield from PS is limited by the restricted rotation of phenyl rings within the extended structure. The conditions outlined herein lead to a 13% yield of phenol from PS, establishing a foundation for future optimization studies that could consider other HAT mediators, initiators, or reaction conditions. The partially oxidized PS polymer obtained following the treatment of PS

https://doi.org/10.1021/jacs.4c18143
J. Am. Chem. Soc. 2025, 147, 8687−8694

under Hock process conditions is an effective substrate for treatment under MC autoxidation conditions to convert the remaining phenyl rings into benzoic acid. Collectively, this study has led to important fundamental and practical outcomes relevant to the chemical recycling of waste plastics.

■ ASSOCIATED CONTENT

Supporting Information

The Supporting Information is available free of charge at https://pubs.acs.org/doi/10.1021/jacs.4c18143.

Experimental details with supplemental notes, characterization data, and NMR spectra (PDF)

Cartesian coordinates of the DFT-optimized structures (XYZ)

■ AUTHOR INFORMATION

Corresponding Authors

Ive Hermans − *Department of Chemistry and Department of Chemical and Biological Engineering, University of Wisconsin−Madison, Madison, Wisconsin 53706, United States; The Wisconsin Energy Institute, University of Wisconsin−Madison, Madison, Wisconsin 53726, United States;* orcid.org/0000-0001-6228-9928; Email: hermans@chem.wisc.edu

Shannon S. Stahl − *Department of Chemistry, University of Wisconsin−Madison, Madison, Wisconsin 53706, United States; The Wisconsin Energy Institute, University of Wisconsin−Madison, Madison, Wisconsin 53726, United States;* orcid.org/0000-0002-9000-7665; Email: stahl@chem.wisc.edu

Authors

Doohyun Baek − *Department of Chemistry, University of Wisconsin−Madison, Madison, Wisconsin 53706, United States; The Wisconsin Energy Institute, University of Wisconsin−Madison, Madison, Wisconsin 53726, United States;* orcid.org/0000-0003-4059-2832

Abdullah J. Al Abdulghani − *Department of Chemical and Biological Engineering, University of Wisconsin−Madison, Madison, Wisconsin 53706, United States;* orcid.org/0000-0002-8560-6209

Dylan J. Walsh − *Department of Chemistry, University of Wisconsin−Madison, Madison, Wisconsin 53706, United States; The Wisconsin Energy Institute, University of Wisconsin−Madison, Madison, Wisconsin 53726, United States;* orcid.org/0000-0001-7981-2770

Dillon T. Hofsommer − *Department of Chemistry, University of Wisconsin−Madison, Madison, Wisconsin 53706, United States; The Wisconsin Energy Institute, University of Wisconsin−Madison, Madison, Wisconsin 53726, United States*

James B. Gerken − *Department of Chemistry, University of Wisconsin−Madison, Madison, Wisconsin 53706, United States;* orcid.org/0009-0000-9294-6300

Changxia Shi − *Department of Chemistry, Colorado State University, Fort Collins, Colorado 80523, United States*

Eugene Y.-X. Chen − *Department of Chemistry, Colorado State University, Fort Collins, Colorado 80523, United States;* orcid.org/0000-0001-7512-3484

Complete contact information is available at: https://pubs.acs.org/10.1021/jacs.4c18143

Notes

The authors declare no competing financial interest.

■ ACKNOWLEDGMENTS

This work was supported by the DOE Office of Science (Office of Basic Energy Sciences) grant DE-SC0023281. The work done at Colorado State University (CSU) was supported by the U.S. Department of Energy, Office of Energy Efficiency and Renewable Energy, Advanced Materials and Manufacturing Technologies Office (AMMTO), and Bioenergy Technologies Office (BETO), performed as part of the BOTTLE Consortium, which includes members from CSU, and funded under contract no. DE-AC36-08GO28308 with the National Renewable Energy Laboratory, operated by the Alliance for Sustainable Energy. NMR spectrometers were supported by the NSF grant CHE-1048642 and by the Great Lakes Bioenergy Research Center (GLBRC) grant DE-SC0018409. Mass spectrometry was supported by the NIH grant 1S10 OD020022-1. We acknowledge the UW-Madison Department of Chemistry HPC Center and the UW-Madison Center for High Throughput Computing (CHTC) for providing computing resources.

■ REFERENCES

(1) Hidalgo-Crespo, J.; Moreira, C. M.; Jervis, F. X.; Soto, M.; Amaya, J. L.; Banguera, L. Circular Economy of Expanded Polystyrene Container Production: Environmental Benefits of Household Waste Recycling Considering Renewable Energies. *Energy Rep.* **2022**, *8*, 306−311.

(2) Tullo, A. H. Plastic Has a Problem; Is Chemical Recycling the Solution? *Chem. Eng. News* **2019**, *97*, 39.

(3) Martín, A. J.; Mondelli, C.; Jaydev, S. D.; Pérez-Ramírez, J. Catalytic Processing of Plastic Waste on the Rise. *Chem* **2021**, *7*, 1487−1533.

(4) Schyns, Z. O. G.; Shaver, M. P. Mechanical Recycling of Packaging Plastics: A Review. *Macromol. Rapid Commun.* **2021**, *42*, 2000415.

(5) Chen, X.; Wang, Y.; Zhang, L. Recent Progress in the Chemical Upcycling of Plastic Wastes. *ChemSuschem* **2021**, *14*, 4137−4151.

(6) Zhang, F.; Wang, F.; Wei, X.; Yang, Y.; Xu, S.; Deng, D.; Wang, Y.-Z. From Trash to Treasure: Chemical Recycling and Upcycling of Commodity Plastic Waste to Fuels, High-Valued Chemicals and Advanced Materials. *J. Energy Chem.* **2022**, *69*, 369−388.

(7) Xu, Z.; Sun, D.; Xu, J.; Yang, R.; Russell, J. D.; Liu, G. Progress and Challenges in Polystyrene Recycling and Upcycling. *ChemSuschem* **2024**, *17*, No. e202400474.

(8) Lopez, G.; Artetxe, M.; Amutio, M.; Alvarez, J.; Bilbao, J.; Olazar, M. Recent Advances in the Gasification of Waste Plastics. A Critical Overview. *Renewable Sustainable Energy Rev.* **2018**, *82*, 576−596.

(9) Peng, Y.; Wang, Y.; Ke, L.; Dai, L.; Wu, Q.; Cobb, K.; Zeng, Y.; Zou, R.; Liu, Y.; Ruan, R. A Review on Catalytic Pyrolysis of Plastic Wastes to High-Value Products. *Energy Convers. Manage.* **2022**, *254*, 115243.

(10) Musa, A.; Jaseer, E. A.; Barman, S.; Garcia, N. Review on Catalytic Depolymerization of Polyolefin Waste by Hydrogenolysis: State-of-the-Art and Outlook. *Energy Fuels* **2024**, *38*, 1676−1691.

(11) Ragaert, K.; Delva, L.; Van Geem, K. Mechanical and Chemical Recycling of Solid Plastic Waste. *Waste Manage.* **2017**, *69*, 24−58.

(12) Oh, S.; Stache, E. E. Recent Advances in Oxidative Degradation of Plastics. *Chem. Soc. Rev.* **2024**, *53*, 7309−7327.

(13) Tomás, R. A. F.; Bordado, J. C. M.; Gomes, J. F. P. P-Xylene Oxidation to Terephthalic Acid: A Literature Review Oriented toward Process Optimization and Development. *Chem. Rev.* **2013**, *113*, 7421−7469.

(14) Partenheimer, W. Valuable Oxygenates by Aerobic Oxidation of Polymers Using Metal/Bromide Homogeneous Catalysts. *Catal. Today* **2003**, *81*, 117−135.
(15) Sullivan, K. P.; Werner, A. Z.; Ramirez, K. J.; Ellis, L. D.; Bussard, J. R.; Black, B. A.; Brandner, D. G.; Bratti, F.; Buss, B. L.; Dong, X.; Haugen, S. J.; Ingraham, M. A.; Konev, M. O.; Michener, W. E.; Miscall, J.; Pardo, I.; Woodworth, S. P.; Guss, A. M.; Román-Leshkov, Y.; Stahl, S. S.; Beckham, G. T. Mixed Plastics Waste Valorization through Tandem Chemical Oxidation and Biological Funneling. *Science* **2022**, *378*, 207−211.
(16) Rabot, C.; Chen, Y.; Lin, S.-Y.; Miller, B.; Chiang, Y.-M.; Oakley, C. E.; Oakley, B. R.; Wang, C. C. C.; Williams, T. J. Polystyrene Upcycling into Fungal Natural Products and a Biocontrol Agent. *J. Am. Chem. Soc.* **2023**, *145*, 5222−5230.
(17) Zhao, B.; Tan, H.; Yang, J.; Zhang, X.; Yu, Z.; Sun, H.; Wei, J.; Zhao, X.; Zhang, Y.; Chen, L.; Yang, D.; Deng, J.; Fu, Y.; Huang, Z.; Jiao, N. Catalytic Conversion of Mixed Polyolefins under Mild Atmospheric Pressure. *Innovation* **2024**, *5*, 100586.
(18) Luo, X.; Zhan, J.; Mei, Q.; Zhang, S. Selective Oxidative Upgrade of Waste Polystyrene Plastics by Nitric Acid to Produce Benzoic Acid. *Green Chem.* **2023**, *25*, 6717−6727.
(19) Ong, A.; Teo, J. Y. Q.; Feng, Z.; Tan, T. T. Y.; Lim, J. Y. C. Organocatalytic Aerobic Oxidative Degradation of Polystyrene to Aromatic Acids. *ACS Sustainable Chem. Eng.* **2023**, *11*, 12514−12522.
(20) Sun, C.; Guo, Y.; Liu, X.; Wang, Y. Heterogeneous Oxidative Upcycling of Polystyrene Plastics to Benzoic Acid under Air Conditions. *Catal. Sci. Technol.* **2024**, *14*, 6584−6591.
(21) Pinsuwan, K.; Phowattanachai, N.; Kaewnoparat, P.; Malakul Na Ayutthaya, A.; Poungboon, T.; Opaprakasit, P.; Petchsuk, A.; Opaprakasit, M. Chemical Recycling of Polystyrene Resin and Its Single-Used Products *via* Nitric Acid Oxidation: Mechanisms and Effects of Other Plastic Contaminations. *Polymer* **2025**, *316*, 127888.
(22) Wang, M.; Wen, J.; Huang, Y.; Hu, P. Selective Degradation of Styrene-Related Plastics Catalyzed by Iron under Visible Light. *ChemSuschem* **2021**, *14*, 5049−5056.
(23) Cao, R.; Zhang, M.-Q.; Hu, C.; Xiao, D.; Wang, M.; Ma, D. Catalytic Oxidation of Polystyrene to Aromatic Oxygenates over a Graphitic Carbon Nitride Catalyst. *Nat. Commun.* **2022**, *13*, 4809.
(24) Huang, Z.; Shanmugam, M.; Liu, Z.; Brookfield, A.; Bennett, E. L.; Guan, R.; Vega Herrera, D. E.; Lopez-Sanchez, J. A.; Slater, A. G.; McInnes, E. J. L.; Qi, X.; Xiao, J. Chemical Recycling of Polystyrene to Valuable Chemicals via Selective Acid-Catalyzed Aerobic Oxidation under Visible Light. *J. Am. Chem. Soc.* **2022**, *144*, 6532−6542.
(25) Oh, S.; Stache, E. E. Chemical Upcycling of Commercial Polystyrene via Catalyst-Controlled Photooxidation. *J. Am. Chem. Soc.* **2022**, *144*, 5745−5749.
(26) Qin, Y.; Zhang, T.; Ching, H. Y. V.; Raman, G. S.; Das, S. Integrated Strategy for the Synthesis of Aromatic Building Blocks via Upcycling of Real-Life Plastic Wastes. *Chem* **2022**, *8*, 2472−2484.
(27) Li, T.; Vijeta, A.; Casadevall, C.; Gentleman, A. S.; Euser, T.; Reisner, E. Bridging Plastic Recycling and Organic Catalysis: Photocatalytic Deconstruction of Polystyrene via a C−H Oxidation Pathway. *ACS Catal.* **2022**, *12*, 8155−8163.
(28) Ghalta, R.; Bal, R.; Srivastava, R. Metal-Free Photocatalytic Transformation of Waste Polystyrene into Valuable Chemicals: Advancing Sustainability through Circular Economy. *Green Chem.* **2023**, *25*, 7318−7334.
(29) Nikitas, N. F.; Skolia, E.; Gkizis, P. L.; Triandafillidi, I.; Kokotos, C. G. Photochemical Aerobic Upcycling of Polystyrene Plastics to Commodity Chemicals Using Anthraquinone as the Photocatalyst. *Green Chem.* **2023**, *25*, 4750−4759.
(30) Oh, S.; Stache, E. E. Mechanistic Insights Enable Divergent Product Selectivity in Catalyst-Controlled Photooxidative Degradation of Polystyrene. *ACS Catal.* **2023**, *13*, 10968−10975.
(31) Ong, A.; Wong, Z. C.; Chin, K. L. O.; Loh, W. W.; Chua, M. H.; Ang, S. J.; Lim, J. Y. C. Enhancing the Photocatalytic Upcycling of Polystyrene to Benzoic Acid: A Combined Computational-Experimental Approach for Acridinium Catalyst Design. *Chem. Sci.* **2024**, *15*, 1061−1067.
(32) During preparation of this article, De Vos and co-workers reported an innovative stepwise process for production of terephthalic acid from PS. See: Giakoumakis, N. S.; Marquez, C.; De Oliveira-Silva, R.; Sakellariou, D.; De Vos, D. E. Upcycling of Polystyrene to Aromatic Polyacids by Tandem Friedel−Crafts and Oxidation Reactions. *J. Am. Chem. Soc.* **2024**, *146*, 34753−34762.
(33) Ghanta, M.; Acharyya, S. S.; Chaudhari, R. V.; Subramaniam, B. Catalytic Aromatic Oxidations. In *Industrial Arene Chemistry*; John Wiley & Sons, Ltd, 2023, pp. 1067−1106.
(34) Suresh, A. K.; Sharma, M. M.; Sridhar, T. Engineering Aspects of Industrial Liquid-Phase Air Oxidation of Hydrocarbons. *Ind. Eng. Chem. Res.* **2000**, *39*, 3958−3997.
(35) Weber, M.; Weber, M.; Kleine-Boymann, M. Phenol. In *Ullmann's Encyclopedia of Industrial Chemistry*; Wiley-VCH, Ed.: 2004.
(36) Fukuda, O.; Sakaguchi, S.; Ishii, Y. Preparation of Hydroperoxides by N-Hydroxyphthalimide-Catalyzed Aerobic Oxidation of Alkylbenzenes and Hydroaromatic Compounds and Its Application. *Adv. Synth. Catal.* **2001**, *343*, 809−813.
(37) Melone, L.; Gambarotti, C.; Prosperini, S.; Pastori, N.; Recupero, F.; Punta, C. Hydroperoxidation of Tertiary Alkylaromatics Catalyzed By N-Hydroxyphthalimide and Aldehydes under Mild Conditions. *Adv. Synth. Catal* **2011**, *353*, 147−154.
(38) Kuhnle, A.; Duda, M.; Tanger, U.; Sheldon, R. A.; Manickam, S.; Arends, I. W. C. E. *Method for Producing Aromatic Alcohols, Especially Phenol*. US 6,720,462 B2, 2004.
(39) Dakka, J. M.; Buchanan, J. S.; Cheng, J. C.; Chen, T.-J.; DeCaul, L. C.; Helton, T. E.; Stanat, J. E.; Benitez, F. M. *Process for Producing Phenol and/or Cyclohexanone*. US 8,247,627 B2, 2012.
(40) Wang, K.; Dakka, J. M. *Process for Producing Phenol*. US 9,029,612 B2, 2015.
(41) All reactions with high pressures of O_2 were limited to small volumes (≤2 mL) with appropriate safety precautions (see section 1c of the Supporting Information). For larger-volume experiments, a dilute oxygen source (6% O_2 in N_2) was used to maintain pO_2 below the limiting oxygen concentrations. See the following for context: Osterberg, P. M.; Niemeier, J. K.; Welch, C. J.; Hawkins, J. M.; Martinelli, J. R.; Johnson, T. E.; Root, T. W.; Stahl, S. S. Experimental Limiting Oxygen Concentrations for Nine Organic Solvents at Temperatures and Pressures Relevant to Aerobic Oxidations in the Pharmaceutical Industry. *Org. Process Res. Dev.* **2015**, *19*, 1537−1543.
(42) The MC-like conditions used here were adopted from ref 15, which achieved a similar yield of benzoic acid when oxidizing PS with a similar M_w. We note that higher benzoic acid yields should be accessible by using the conventional Co/Mn/Br MC conditions, which require specialized equipment (see ref 14, for context).

https://doi.org/10.1021/jacs.4c18143
J. Am. Chem. Soc. 2025, 147, 8687−8694